Journal of Medicinal Chemistry

Article

pubs.acs.org/jmc

Identification of Novel Adenosine A_{2A} Receptor Antagonists by Virtual Screening

Christopher J. Langmead,*[,†] Stephen P. Andrews,[†] Miles Congreve,[†] James C. Errey,[†] Edward Hurrell,[†] Fiona H. Marshall,[†] Jonathan S. Mason,[†] Christine M. Richardson,[‡] Nathan Robertson,[†] Andrei Zhukov,[†] and Malcolm Weir[†]

[†]Heptares Therapeutics Limited, BioPark, Broadwater Road, Welwyn Garden City, Hertfordshire AL7 3AX, U.K.

[‡]BioFocus, Great Chesterford Research Park, Saffron Walden, CB10 1XL, U.K.

Supporting Information

ABSTRACT: Virtual screening was performed against experimentally enabled homology models of the adenosine A_{2A} receptor, identifying a diverse range of ligand efficient antagonists (hit rate 9%). By use of ligand docking and Biophysical Mapping (BPM), hits **1** and **5** were optimized to potent and selective lead molecules (**11**–**13** from **5**, pK_I = 7.5–8.5, 13- to >100-fold selective versus adenosine A_1; **14**–**16** from **1**, pK_I = 7.9–9.0, 19- to 59-fold selective).

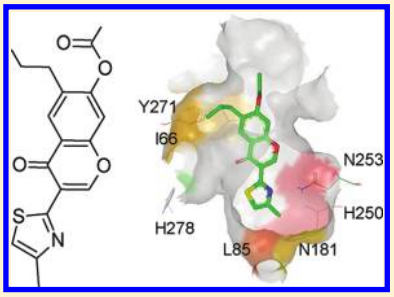

INTRODUCTION

The adenosine A_{2A} receptor is a member of the G-protein-coupled receptor (GPCR) superfamily that mediates effects of the purine nucleotide adenosine on cellular signaling. The receptor is expressed in the CNS and periphery and has been a long-standing drug target for the treatment of inflammatory disorders and Parkinson's disease. The A_{2A} receptor is expressed in midbrain regions of the CNS where it functionally opposes the actions of the dopamine D_2 receptor. Given that the primary pathology in Parkinson's disease is a loss of dopamine and hence reduced dopamine D_2 receptor activation, adenosine A_{2A} receptor antagonism represents a potential nondopaminergic therapy for this disorder. Initial work to identify antagonists focused on purine and xanthine derivatives, essentially based on adenosine and the naturally occurring antagonist caffeine. This class of compounds is exemplified by istradefylline[1] (KW-6002), which progressed to phase III clinical development; however, despite extensive efforts, no other clinical agents that selectively target the A_{2A} receptor have emerged from this area of chemistry. Further work has focused on bicyclic and tricyclic derivatives such as triazolotriazines and triazolopyrimidines, exemplified by ZM241385 and vipadenant, respectively.[1] The most advanced of this class of compounds is preladenant, which is currently in phase III clinical trials.[1] However, despite good affinity and selectivity across other adenosine receptor subtypes, these compounds are generally high molecular weight and all contain a furan group that has proven difficult to replace by empirical medicinal chemistry. Such an electron-rich group is prone to oxidative metabolism and potential reactive metabolite formation.[2] Therefore, we sought an alternative structure-based approach to identify novel antagonist chemotypes for the adenosine A_{2A} receptor. By use of an experimentally enabled (site-directed mutagenesis, SDM) homology model of the receptor (based on the crystal structure of the turkey β_1 adrenergic receptor in complex with cyanopindolol[3]), a virtual screen was performed to attempt to identify novel hits. In silico screening of 545K compounds, filtered to focus on compounds with CNS druglike properties and without undesirable heterocycles such as the furan or xanthine moieties, resulted in 20 confirmed hits in vitro (9% hit rate). These hits included a highly potent 1,3,5-triazine derivative and a chromone scaffold, the latter a completely novel chemotype for adenosine receptors. The binding modes of these hits were refined using our Biophysical Mapping approach, allowing optimal interactions to be identified and enabling these compounds to be rapidly developed into potent antagonists suitable for further optimization.[4]

RESULTS AND DISCUSSION

Virtual Screening. At the time of this work, no structural data were available for the A_{2A} receptor, and therefore homology models were constructed based on the avian β_1 adrenergic GPCR crystal structure bound to cyanopindolol (PDB code 2VT4).[3] Several different computational methods were used to generate and validate two homology models (see methods section and Supporting Information) because there is relatively low percentage identity between the two proteins (25% overall, <20% around the putative ligand binding site). The validation step included an assessment of the consistency in the alignments and of the variability, including which regions of the models had higher and lower confidence associated with

Received: October 12, 2011
Published: January 17, 2012

them. The helical bundles between the two models and the template agreed closely, with lower confidence in the loop regions, particularly the extracellular loop 2, which did not align well to the template. By use of published and in-house SDM data to validate and improve the models and docking experiments using Glide[5] of a small number of known A_{2A} receptor ligands and similarly sized decoys, virtual screening conditions and protocols were established. A discussion of the SDM data used to improve the models has been described elsewhere and is summarized in the methods section.[4] A comparison of the homology modeling results with ligand-complexed crystal structures of the adenosine A_{2A} receptor is detailed in ref 6.

Virtual screening was then carried out with compound data sets of commercially available compounds, filtered to focus on compounds with desired CNS druglike properties. 545 000 compounds were prepared for screening, and all or a more filtered and clustered set were docked into each of the models using the SP algorithm within the Glide software, running on a 28 CPU Linux cluster. Details of the workflows, screening compound numbers and filters used for the virtual screening, and postprocessing analyses with each homology model are detailed in the Supporting Information (Figures S2–S4). The aim of the screen was to identify novel chemotypes that would provide starting points for optimization to compounds with good druglike properties. A number of different protocols were used to analyze the output from the virtual screens to provide a set of complementary compound selections, each biased toward certain features of the binding site; in each case, up to 10–20000 ligand poses were initially selected based on the score from Glide. This data set was then sectioned in various ways including the use of consensus scoring, use of other Glide generated scores, and overlap with the docked poses of known small ligands for the receptor. It was of particular interest to assess the utility of the SDM data in guiding compound selections. Therefore, most of the compounds were selected based on balanced polar and lipophilic score components and proximity to one or more residues chosen based on the experimental (SDM) data. As part of this process, a bias was employed to focus on compounds that docked in the most buried part of the site, remote from the low confidence region bordered by the extracellular loop 2. Compound sets resulting from the various selections were combined, and a final selection was made involving 3D visualization and assessment in the binding site, including the fit to the binding site shape and key features and the ligand conformation, and final triage by medicinal chemistry. As a result of this process, a set of 372 compounds was prioritized. Of these, only 230 were logistically available commercially and were tested for in vitro binding to the adenosine A_{2A} receptor. Twenty compounds exhibited activity (IC_{50} < 55 μM), giving a 9% hit rate overall. Of the top 10 hits, all have ligand efficiencies (LEs) of >0.27, with seven compounds having >0.3, three having >0.4, and one notable hit with LE > 0.5.[7] These best hits also have reasonable to good ligand lipophilicity efficiencies (LLEs) in the range 2.1–5.4, with eight having LLE ≥ 3.[8] A number of structurally distinct chemotypes were identified in the screen, providing multiple starting points for potential optimization to generate a new A_{2A} antagonist series: Table 1 and Figure 1 indicate the top 10 hits ranked by LE. Full binding curves for these hits are shown in the Supporting Information, which includes a table of the nearest published adenosine A_{2A} antagonist to each of the hits. The most potent and most efficient compounds were all identified by the protocols that used key interacting residues from the SDM data as part of the selection process. This study highlights the importance of using experimental data, where available, in analysis and virtual hit selection during a virtual screen.

Table 1. Virtual Screening Hits

hit	pK_I	LE	LLE	clogP	PSA	MW
1	8.46	0.52	5.4	3.1	84.9	310.4
2	5.15	0.47	4.5	0.7	72.2	222.3
3	5.75	0.44	3.9	1.9	61.7	264.3
4	6.15	0.36	3.2	3.0	66.6	327.4
5	5.65	0.33	3.7	1.9	85.7	331.3
6	5.62	0.31	2.6	3.0	76.7	367.9
7	5.91	0.30	3.2	2.7	78.4	367.4
8	5.33	0.29	3.4	1.9	79.8	340.4
9	5.70	0.29	3.9	1.8	80.1	363.4
10	5.53	0.27	2.1	3.4	95.9	382.4

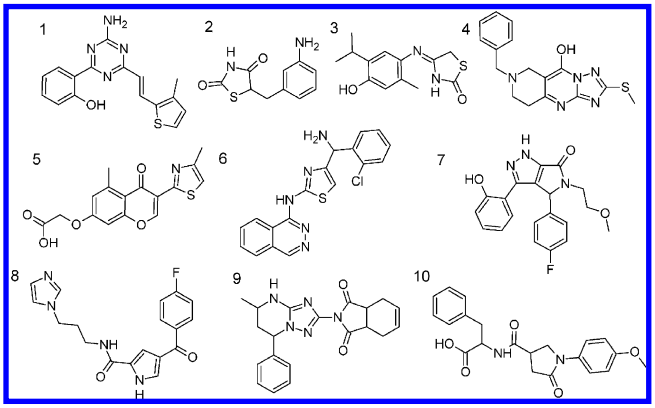

Figure 1. Structures of virtual screening hits.

The results from this virtual screening exercise have demonstrated that good hit rates of diverse leadlike compounds are possible using high-quality GPCR (experimentally enabled and enhanced) homology models. The utility of virtual screening is supported by two recent papers from academic labs documenting this approach using an X-ray structure (rather than a homology model) of the adenosine A_{2A} receptor.[9,10] One group reported that a hit rate of 41% was achieved with 23 of the 56 assayed compounds showing activity better than 10 μM.[9] Similarly a second study yielded a hit rate of 35% with 7 of 20 compounds tested having affinities from 200 nM to 10 μM.[10] Interestingly, the top ranked hit from one of these two screens contains the same chemical scaffold as observed here from virtual screening of our experimentally enhanced homology model.[9]

Hits to Leads. The process for the selection and optimization of the initial hits to develop leads was driven from docked ligand poses into the A_{2A} homology models, coupled with 3D analysis of hotspots in the binding site, which were determined using small fragment probes. The calculated GRID maps[11] especially showed clearly the shape and pharmacophoric preferences/constrictions of the binding site (using a methyl group for shape and an aromatic C–H group, a carbonyl group, and an amide NH group for lipophilic, hydrogen-bond acceptor and donor hotspots, respectively). The relatively high LE and LLE of the hits indicate that the A_{2A} receptor binding site is quite druggable, and this is reinforced by the GRID analysis suggesting regions of hydrophobic and H-

dx.doi.org/10.1021/jm201455y | J. Med. Chem. 2012, 55, 1904–1909

Scheme 1. Optimization of Chromone Hit 5

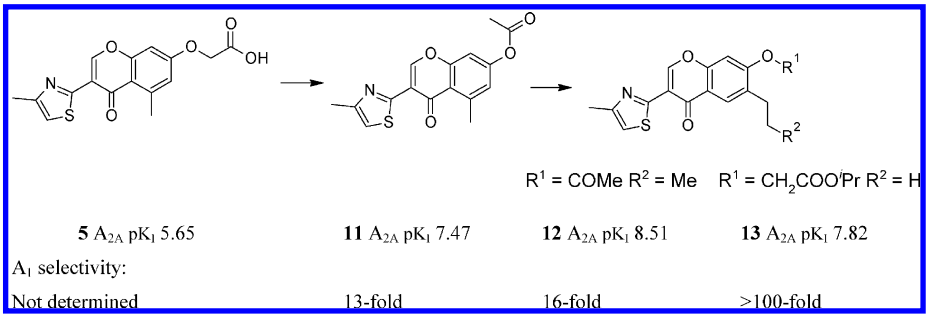

bonding hotspots close together in the site available for very small ligands to bind. The key H-bonding residue Asn253$^{6.55}$ sits centrally and is capable of forming high quality interactions with a diverse range of heterocyclic compounds. In particular, two hits were rapidly developed into lead series with potent activity versus the A_{2A} receptor and good selectivity in key examples against the adenosine A_1 receptor. Introducing at least moderate selectivity versus the A_1 receptor subtype was thought desirable to minimize potential side effects, such as the stimulant effects seen with nonselective agents such as caffeine. The A_{2A} binding site was also analyzed using molecular dynamics simulations with the WaterMap software (Schrödinger),[12] shown in ref 6, which demonstrates that our highly ligand efficient ligands occupy exactly the region where there is a cluster of waters that are termed "unhappy", meaning that energetically they would prefer to be in bulk solvent; this contrasts with larger ligands such as ZM241385.[13]

The first hit to be optimized was the chromone **5** (Figure 1, Scheme 1). Selection of closely related analogues from commercial suppliers, influenced by the proposed binding mode from the virtual docking, quickly identified several more potent compounds including ester **11**. In particular, relatively close analogues lacking the carboxylic acid functionality (presumed to be undesirable for brain penetration) and also not significantly higher in molecular weight or lipophilicity were selected. Biophysical Mapping analysis, published elsewhere[4] (chromone analogues are **1** in the earlier publication), distinguished between the binding mode shown in Figure 2 and a pose in which the compounds were rotated 180° and interacted with the key Asn253$^{6.55}$ via the chromone carbonyl.[4]

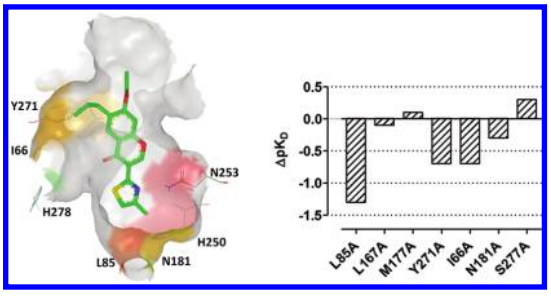

Figure 2. Docking of the chromone **12**, showing the BPM fingerprint color coded onto the binding site residues and in graphical form as change in pK_D. Nonbinding is shown in red (N253A, H250A). Next largest effect is in dark orange (L85A), second largest in amber (N181A, Y271A, I66A), an increase in binding in green (S277A). H-bonding between the nitrogen of the thiazole and the aromatic C−H of the chromone is predicted to Asn253$^{6.55}$. Selected BPM data are tabulated showing the change in pK_D of each binding site mutation.

Further iterations of purchasing of close analogues of **11** identified **12** and **13** that are highly potent and, in the case of **13**, highly selective A_{2A} antagonists. In addition to the BPM data, a low resolution crystal structure of one member of the series was solved confirming the binding pose presented here (data not shown). Despite rapid progress with this series, in vitro metabolism issues and concerns that the thiazole might represent a liability in terms of possible generation of reactive metabolites led us to halt work in this series. Indeed, many previous adenosine A_{2A} antagonists carry a furan group and we reasoned that a superior class of compounds should not contain a similar liability.[1] In addition, the potential of the work in the triazine scaffold (below and in ref 6) allowed us to deprioritize the chromone template.

The second series to be optimized was triazine **1** (Scheme 2), already a highly potent A_{2A} antagonist with excellent LE and LLE.[7,8] Simple outline SAR established the importance of the amino and phenol functionalities for high potency (data not shown) and that the olefin could be replaced by a range of groups, including simplification to alkyl-substituted **14**. This fragment-sized molecule retains much of the affinity for the receptor and has moderate selectivity over the A_1 receptor. A range of derivatives were synthesized in a hits to leads program on the chemotype, and one direction of the work was to design phenyl substituted **15** and **16** containing piperazine and piperidine solubilizing groups. These derivatives were found to be highly potent antagonists with moderate to good selectivity. BPM analysis of this series of compounds was again used during the optimization process, and a representative data set is shown in Figure 3 and is described in the legend. One further area of optimization of the series was to examine modifications to the triazine scaffold itself to allow more direct access to the "ribose pocket" from which we believed selectivity over the A_1 receptor could be derived. This is the topic of ref 6.

Comparisons can be made of the binding modes of the chromone and triazine templates using BPM analysis. Alanine mutation of Asn253$^{6.55}$ or His250$^{6.52}$ abolished the binding of **12** and **15**; ligand docking suggested that Asn253$^{6.55}$ makes key hydrogen bonding interactions with the amino and phenol functional groups of **15** while for **12** the interaction with Asn253$^{6.55}$ is made by the aromatic C−H of the chromone template and the nitrogen atom of the thiazole substituent. Alanine mutation of Ile66$^{2.64}$ (ΔpK_D = −0.7) and Tyr271$^{7.36}$ (ΔpK_D = −0.7) reduced the affinity of **12**, consistent with these residues forming a pocket for the alkyl chain of this compound. However, these mutations had little or no effect on the binding of **15** (ΔpK_D of +0.1 and −0.1, respectively). Conversely, alanine mutation of Ser277$^{7.42}$ reduced the affinity of **15** (ΔpK_D = −1.0) but not **12** (ΔpK_D = +0.3), consistent with the piperazine group of **15** being oriented toward the pocket of the

dx.doi.org/10.1021/jm201455y | J. Med. Chem. 2012, 55, 1904−1909

Scheme 2. Optimization of Triazine Hit 1

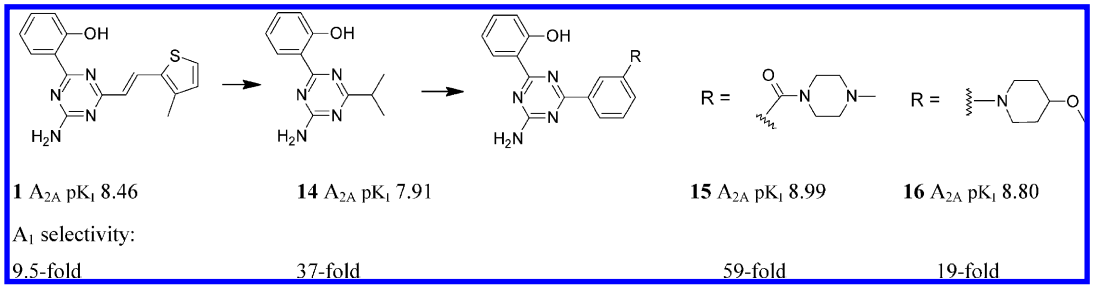

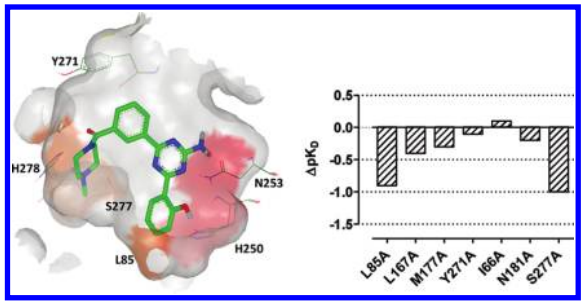

Figure 3. Docking of the triazine **15**, showing the BPM fingerprint color coded onto the binding site residues and in graphical form as change in pK_D. Nonbinding is shown in red (N253A, H250A). Next largest effect is in dark orange (L85A, S277A). H-bonding between the nitrogen of the triazine and the phenol is predicted to Asn253[6.55]. The polar piperazine substituent is proposed to reach into the region of the binding site occupied by ribose in the natural agonist ligand adenosine and may be the driver of selectivity versus the A_1 receptor, as this region of the binding site contains some amino acid differences comparing the two receptors.[14] Selected BPM data are tabulated showing the change in pK_D of each binding site mutation.

receptor occupied by the ribose group of adenosine. The rationalization of the binding modes of these two chemotypes represents the first application of BPM analysis[4] to lead generation and has enabled the progression of this chemistry into lead optimization and beyond.[6]

CONCLUSION

The advent of improved homology modeling and the increasing availability of structural data for GPCRs are now enabling virtual screening for receptor targets to be used as a viable alternative to high-throughput screening. In this study we aimed to identify novel adenosine A_{2A} antagonists through virtual screening of a library of 545K compounds using a homology model based on the turkey β_1 adrenoceptor. Hits were computationally filtered and then cherry picked for screening, taking into account properties of the binding site (shape, electronic), the ligand (conformation), and desired regions for interaction (SDM data), leading to a 9% hit rate from 230 compounds tested by competition radioligand binding. Of the top 10 hits, 7 had good LE (>0.3) and LLE (>3), suggesting that they may represent suitable starting points for further optimization. Notably, one of the hits was a chromone (**5**), a chemotype completely novel in the field of adenosine receptors antagonists. Using ligand docking and Biophysical Mapping, latterly supported by X-ray structure determination, we have been able to identify a credible ligand binding model.[4] A series of optimal ligands that displayed greatly improved affinities compared to **5** and selectivity over the adenosine A_1 receptor subtype were discovered. However, other in vitro properties made this series unsuitable for further optimization. The top ranked hit from the screen, containing a 1,3,5-triazine core, was by far the most potent, with LE > 0.5 and LLE > 5 and an affinity of <10 nM for the A_{2A} receptor. Notably, this core group was also identified in a separate virtual screening exercise for the A_{2A} receptor using an X-ray structure.[9] SAR in this series demonstrated the importance of the amino and phenol groups, but the olefin moiety could be readily replaced by a simple alkyl substituent with minimal loss of affinity. Such a potent, low molecular weight compound made an excellent starting point for optimization. Further analogues were designed using a binding model determined using Biophysical Mapping, to exploit the "ribose pocket" within the receptor to improve affinity and selectivity over the A_1 receptor. This process resulted in several highly potent analogues with favorable selectivity profiles, suitable for further optimization. Continued exploitation of the results presented in this article is the subject of ref 6.

EXPERIMENTAL PROTOCOLS

Virtual Screening Compounds. The compounds used for the virtual screening were from CAP,[15] a collection of commercial vendor catalogues, together with a subset of the BioFocus SoftFocus library collections. The hits shown were provided by Chembridge (**1**, **5**), Interchim (**2**, **3**, **8**, **9**), Asinex (**4**), Inter-bioscreen (**7**, **10**), and BioFocus (**6**).

Computational Chemistry. Homology models were constructed from the avian β_1 adrenergic GPCR crystal structure bound to cyanopindolol (PDB code 2VT4).[3,16] Owing to the relatively low percentage identity between the two proteins (25% overall, <20% around the ligand binding site), two initial homology models of the adenosine A_{2A} receptor were generated, using different methods. This provided a means to assess consistency in the alignments, the variability within the built structures, and which regions of the models had higher and lower confidence associated with them. One model was constructed using MODELLER,[17,18] while the other was constructed using MOE[19] with manual readjustment of the ClustalW alignment where necessary.[20] The alignment in each case was checked to ensure consistency with known GPCR conserved motifs[21] and particularly the conserved disulfide bond, common to family A GPCRs, which is located between the top of helix 3 and the extracellular loop 2. Apart from the extracellular loop 2, the rest of the modeled structures showed good agreement and in the MOE model this loop was not modeled beyond the first few residues up to and including Phe168 because of the very poor alignment in this region. The two homology models were then further evaluated using two different approaches. First, SDM data, both from the literature[22] and in-house,[4] were mapped onto the modeled protein structures. The majority of these residues lined the anticipated ligand binding site in each of the models. The mutation sites showed good consistency in the locations of the residues when comparing the two structures. Second, both models were used to dock a small number of known A_{2A} antagonists, including ZM241385, into each of the structures using Glide as the docking engine.[5,23] This was done to explore the potential docking modes that

dx.doi.org/10.1021/jm201455y | J. Med. Chem. 2012, 55, 1904−1909

could be achieved and to assist in the development of conditions and protocols for use in analysis of the virtual screen, with similarly sized decoys also being used in the studies. It was decided to use the two models in parallel in the virtual screen.

Ligand data sets were drawn from CAP,[15] a collection of vendor catalogues giving details of screening samples for purchase. A subset of the BioFocus SoftFocus library collections were also screened after excluding compounds designed to target GPCRs. The compounds from CAP were prefiltered to remove those molecules containing unwanted chemical functionality. Physicochemical profiles for the data set were biased toward a CNS-like profile based on the recommendations in Pajouhesh et al.[24] and the properties of a set of literature A_{2A} antagonists. 545K compounds were prepared for screening, and all or a subset from more stringent prefiltering and clustering docked into each of the models using the SP algorithm within the Schrödinger Glide software, running on a 28 CPU Linux cluster. Details of the workflows, screening compound numbers, and filters used for the virtual screening and postprocessing analyses with each homology model are detailed in the Supporting Information (Figures S2−S4). The protein preparation and docking experiments were done within the Schrödinger Maestro package. The grid generation necessary for docking was done within Glide. The residues highlighted in SDM experiments (in-house and external) were used to further define the cavity of the grid. However, no constraints were added in the grid generation to ensure that subsequent dockings were not biased in any way. As standard, up to 3 poses per molecular structure were stored for analysis. For some compound subsets, Glide XP docking was carried out on the ligands with 10 poses per ligand being stored. A selection of 372 virtual hits was finally prioritized for purchasing, following manual inspection and subsequent triaging by medicinal chemistry of the most promising docking solutions.

Subsequent docking experiments on the hits from the radioligand binding assay and also on analogues of the two hit chemotypes derived from **1** and **5** were carried out. They were guided by ligand SAR, an iterative process of assessing SDM data, and also by designing our own BPM mutants to confirm or rule out possible binding modes, as previously described.[4] As part of this, more detailed modeling work was carried out, including the use of induced fit docking and restrained minimization work. For the more active compounds, the MOE derived model gave more plausible results, and therefore, this was used as the basis for further improvement and validation work. In particular, validation and improvement of the homology models for docking were conducted, focused on ZM241385, because of the wealth of SAR for this series and the amount of SDM data available for the ligand at the adenosine A_{2A} receptor.[22,25] The induced fit docking (IFD) protocol[23] was used within Maestro with an autogenerated box size around the residues highlighted by SDM as having a large effect on antagonist binding, namely, Ile66$^{2.64}$, Val84$^{3.32}$, Leu85$^{3.33}$, Glu151^{ECL2}, Leu167^{ECL2}, Glu169^{ECL2}, Asn181$^{5.42}$, Phe182$^{5.43}$, His250$^{6.52}$, Asn253$^{6.55}$, Phe257$^{6.59}$, Tyr271$^{7.36}$, Ile274$^{7.39}$, and His278$^{7.43}$.

Adenosine Receptor Assays. Inhibition binding assays were performed using 2.5 μg of membranes prepared from HEK293 cells transiently transfected with human adenosine A_{2A} receptor or 10 μg of membranes prepared from CHO cells stably transfected with human adenosine A_1 receptor. Membranes were incubated in 50 mM Tris-HCl (HEK293-hA_{2A}, pH 7.4) or 20 mM HEPES, 100 mM NaCl, 10 mM $MgCl_2$ (CHO-hA_1, pH 7.4) in the presence of 5−10 concentrations of test compound and 1 nM [^{3}H]ZM241385 (HEK293-hA_{2A}) or [^{3}H]DPCPX (CHO-hA_1) at 25 °C for 1 h. The DMSO concentration was 0.1% (final). The assay was then terminated by rapid filtration onto GF/B grade Unifilter plates using a TomTec cell harvester, followed by 5 × 0.5 mL washes with doubly distilled H_2O. Total binding was defined in the presence of 0.1% DMSO; nonspecific binding was defined in the presence of 1 μM CGS15943 (HEK293-hA_{2A}) or 1 μM DPCPX (CHO-hA_1). Bound radioactivity was determined by liquid scintillation counting, and inhibition curves were analyzed using a four-parameter logistic equation. IC_{50} values were converted to K_I values with the Cheng−Prusoff equation using a K_D derived from saturation binding studies. Compounds were tested to at least $n = 2$; concentration response curves displayed Hill slopes not significantly different from unity, consistent with a competitive mode of action.

Chemical Synthesis. Hit compounds **1**−**10** and follow-up compounds **11**−**14** were provided by Chembridge, Interchim, Asinex, Interbioscreen, or BioFocus. The compounds were supplied with LCMS purities of >95%, as determined by the vendors. Quality control data are provided in the Supporting Information. Chemical synthesis and analysis of **15** and **16** were carried out at Oxygen Healthcare, India, according to Scheme 3. Full experimental details can be found in the Supporting Information.

Scheme 3. Synthesis of 15 and 16[a]

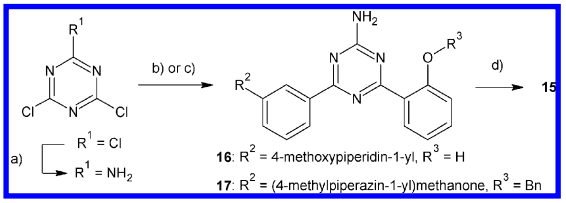

[a]Reagents and conditions: (a) THF, ^{i}Pr$_2$EtN, NH_3. (b) For **16**: (i) 3-(4-methoxypiperidin-1-yl)phenylboronic acid, Na_2CO_3, 1,4-dioxane/H_2O, $Pd(PPh_3)_4$, 90 °C, then (ii) 2-hydroxylphenylboronic acid, Na_2CO_3, 1,4-dioxane/H_2O, $Pd(PPh_3)_4$, 90 °C. (c) For **17**: (i) 2-benzyloxyphenylboronic acid, Na_2CO_3, 1,4-dioxane/H_2O, $Pd(PPh_3)_4$, 70 °C, then (ii) 3-(4-methylpiperazine-1-carbonyl)phenylboronic acid hydrochloride, Na_2CO_3, 1,4-dioxane/H_2O, $Pd(PPh_3)_4$, 90 °C; (d) **17**, EtOAc, $Pd(OH)_2$/C, 1,4-cyclohexadiene, 140 °C (microwave).

■ ASSOCIATED CONTENT

Supporting Information

Chemical synthesis protocols, QC data and binding curves for the top 10 hits, more detailed computational methods including virtual screening workflows, and a table of calculated blood−brain barrier prediction and the closest published adenosine A_{2A} antagonist to each of the hits. This material is available free of charge via the Internet at http://pubs.acs.org.

■ AUTHOR INFORMATION

Corresponding Author

*Phone: +44 (0)1707 358631. Fax: +44 (0)1707 358640. E-mail: chris.langmead@heptares.com.

■ ACKNOWLEDGMENTS

The authors thank Bissan Al-Lazikani for help with constructing the first generation of homology models, Benjamin Tehan for assistance with computational chemistry, and Nat Monck for assisting with the triaging of screening hits.

■ ABBREVIATIONS USED

BPM, Biophysical Mapping; PDB, Protein Data Bank; LE, ligand efficiency; LLE, ligand lipophilicity efficiency; SDM, site directed mutagenesis

■ REFERENCES

(1) Pinna, A. Novel investigational adenosine A_{2A} receptor antagonists for Parkinson's disease. *Expert Opin. Invest. Drugs* **2009**, *18*, 1619−1631.

(2) Blagg, J. Structural Alerts for Toxicity. In *Burger's Medicinal Chemistry, Drug Discovery and Development*, 7th ed.; Abraham, D. J., Rotella, D. P., Eds.; Wiley: Hoboken, NJ, 2010; pp 301−344.

(3) Warne, A.; Serrano-Vega, M. J.; Baker, J. G.; Moukhametzianov, R.; Edwards, P. C.; Henderson, R.; Leslie, A. G. W.; Tate, C. G.;

Schertler, G. F. X. Structure of the beta1-adrenergic G protein-coupled receptor. *Nature* **2008**, *454*, 486−491 (PDB code 2VT4).
(4) Zhukov, A.; Andrews, S. P.; Errey, J. C.; Robertson, N.; Tehan, B.; Mason, J. S.; Marshall, F. H.; Weir, M.; Congreve, M. Biophysical Mapping of the adenosine A_{2A} receptor. *J. Med. Chem.* **2011**, *54*, 4312−4323.
(5) Halgren, T. A.; Murphy, R. B.; Friesner, R. A.; Beard, H. S.; Frye, L. L.; Pollard, W. T.; Banks, J. L. Glide: a new approach for rapid, accurate docking and scoring. 2. Enrichment factors in database screening. *J. Med. Chem.* **2004**, *47*, 1750−1759.
(6) Congreve, M.; Andrews, S. P.; Dore, A. S.; Hollenstein, K.; Hurrell, E.; Langmead, C. J.; Mason, J. S. ; Ng, I. W.; Tehan, B.; Zhukov, A.; Weir, M.; Marshall, F. H. Discovery of 1,2,4-triazine derivatives as adenosine A_{2A} antagonists using structure based drug design. *J. Med. Chem.* [Online early access]. DOI: 10.1021/jm201376w. Published Online: Jan 5, **2012**.
(7) Hopkins, A. L.; Groom, C. R.; Alex, A. Ligand efficiency: a useful metric for lead selection. *Drug Discovery Today* **2004**, *9*, 430−431.
(8) Leeson, P. D.; Springthorpe, B. The influence of drug-like concepts on decision-making in medicinal chemistry. *Nat. Rev. Drug Discovery* **2007**, *6*, 881−890.
(9) Katritch, V.; Jaakola, V.-P.; Lane, J. R.; Lin, J.; Izerman, A. P.; Yaeger, M.; Kufarena, I.; Stevens, R. C.; Abagyan, R. Structure-based discovery of novel chemotypes for adenosine A2a receptor antagonists. *J. Med. Chem.* **2010**, *53*, 1799−1809.
(10) Carlsson, J.; Yoo, L.; Gao, Z. G.; Irwin, J. J.; Shoichet, B. K.; Jacobson, K. A. Structure-based discovery of A_{2A} adenosine receptor ligands. *J. Med. Chem.* **2010**, *53*, 3748−3755.
(11) Goodford, P. J. A computational procedure for determining energetically favorable binding sites on biologically important macromolecules. *J. Med. Chem.* **1985**, *28* (7), 849−857.
(12) Higgs, C.; Beuming, T.; Sherman, W. Hydration site thermodynamics explain SARs for triazolylpurines analogues binding to the A_{2A} receptor. *ACS Med. Chem. Lett.* **2010**, *1*, 160−164.
(13) Congreve, M.; Langmead, C. J.; Mason, J. S.; Marshall, F. H. Progress in structure based drug design for G protein-coupled receptors. *J. Med. Chem.* **2011**, *54*, 4283−4311.
(14) Lebon, G.; Warne, T.; Edwards, P. C.; Bennett, K.; Langmead, C. J.; Leslie, A. G. W.; Tate, C. G. Agonist-bound adenosine A2A receptor structures reveal common features of GPCR activation. *Nature* **2011**, *474*, 521−523.
(15) "Chemicals Available for Purchase" database. Available from http://www.accelrys.com.
(16) Berman, H. M; Westbrook, J.; Feng, Z.; Gilliland, G.; Bhat, T. N.; Weissig, H.; Shindyalov, I. N.; Bourne, P. E. The Protein Data Bank. *Nucleic Acids Res.* **2000**, *28*, 235−242 (http://www.rcsb.org/pdb/static.do?p=general_information/about_pdb/policies_references.html).
(17) Sali, A.; Blundell, T. L. Comparative protein modeling by satisfaction of spatial restraints. *J. Mol. Biol.* **1993**, *234*, 779−815.
(18) Eswar, N.; Marti-Renom, M. A.; Webb, B.; Madhusudhan, M. S.; Eramian, D.; Shen, M.; Pieper, U.; Sali, A. Comparative Protein Structure Modeling with MODELLER. *Current Protocols in Bioinformatics*; Wiley: New York, 2006; Suppl. 15, pp 5.6.1−5.6.30.
(19) *Molecular Operating Environment (MOE)*, version 2008.10; Chemical Computing Group, Inc.: Montreal, Quebec, Canada, 2008; www.chemcomp.com.
(20) Thompson, J. D.; Higgins, D. G.; Gibson, T. J. CLUSTAL W: improving the sensitivity of progressive multiple sequence alignment through sequence weighting, position-specific gap penalties and weight matrix choice. *Nucleic Acids Res.* **1994**, *22*, 4673−4680.
(21) Mirzadegan, T.; Benko, G. Sequence analyses of G-protein coupled receptor: similarities to rhodopsin. *Biochemistry* **2003**, *42* (10), 2759−2767.
(22) Kim, J.; Wess, J.; van Rhee, M.; Schoneberg, T.; Jacobson, K. A. Site-directed mutagenesis identifies residues involved in ligand recognition in the human A_{2A} adenosine receptor. *J. Biol. Chem.* **1995**, *270* (23), 13987−13997.
(23) Available from Schrödinger, LLC, New York (http://www.schrodinger.com).
(24) Pajouhesh, H.; Lenz, G. R. Medicinal chemical properties of successful central nervous system drugs. *NeuroRx* **2005**, *2* (4), 541−553.
(25) Dal Ben, D.; Lambertucci, C.; Marucci, G.; Volpini, R.; Cristalli, G. Adenosine Receptor modeling: What does the A_{2A} crystal structure tell us? *Curr. Top. Med. Chem.* **2010**, *93*, 993−1018.